Observations of the Directional Spectrum of Ocean Waves Using a Cloverleaf Buoy

HISASHI MITSUYASU, FUKUZO TASAI, TOSHIRO SUHARA, SHINJIRO MIZUNO, MAKOTO OHKUSU, TADAO HONDA AND KUNIO RIKIISHI

Research Institute for Applied Mechanics, Kyushu University, Fukuoka, Japan

(Manuscript received 26 August 1974, in revised form 24 April 1975)

ABSTRACT

Analysis of the directional spectra of typical sets of surface wave data obtained in the open sea as well as a bay using a cloverleaf buoy system are reported.

It is shown that the directional wave spectrum can be approximated by the product of the frequency spectrum and a unimodal angular distribution with mean direction approximately equal to that of the wind, and that various forms of frequency spectra exist, even in relatively simple wave systems, depending on their generating conditions. Ocean waves at fairly short dimensionless fetches show spectral forms with very narrow spectral width, which are similar to those of laboratory wind waves. On the other hand, the spectral forms for ocean waves at very long dimensionless fetches are quite similar to the Pierson-Moskowitz spectra, which are considered, within our present data, to be the wave spectra with the largest spectral width. Finally, there exist many ocean waves at moderate dimensionless fetches, which show spectral forms with interminate spectral widths lying between the above two extremes. However, a definite relationship between the spectral width and the dimensionless fetch has not been obtained in the present study.

Concerning the angular distribution, it is shown that the shape of the angular distribution is dependent on the frequency of the spectral component even in a simple wave system in a generating area, although the mean directions of the spectral components are independent of the frequency and approximately equal to the wind direction. The angular distribution is very narrow for frequencies near the dominant peak of the frequency spectrum, whereas it widens rapidly toward high and low frequencies. Thus, the major energy-containing frequency components propagate in almost the same direction as the wind with the least angular spreading.

Finally, it is shown that a similarity law is satisfied for the angular distributions, and an idealized form of the angular distribution function is derived for practical purposes.

1. Introduction

Studies of two-dimensional spectra of ocean waves are very important not only for such practical purposes as wave forecasting but also for clarifying the fundamental process of wave generation. In contrast with a great many studies of the one-dimensional (frequency) spectrum, only a few studies have been made of the two-dimensional (directional) spectrum of ocean waves. Particularly, reliable data for estimating directional spectra of ocean waves are remarkably lacking except for the data reported by Coté *et al.* (1960), Longuet-Higgins *et al.* (1963), Ewing (1969), and recently by Tyler *et al.* (1974).

Since 1971 a group of scientists at the Research Institute for Applied Mechanics, Kyushu University, has conducted a special project on ocean waves which includes fundamental studies on ocean waves and their engineering applications (Mitsuyasu *et al.*, 1973a b). One of the important aims of this project has been an investigation of the directional spectrum of ocean waves under various conditions in order to throw light on the fine-structure of ocean waves and the processes of wave generation.

From 1971–74 seven cruises were made to measure the directional spectrum of ocean waves by using a cloverleaf buoy. Typical wave data measured both in open seas and in a bay have been analyzed to clarify the fundamental properties of the directional spectrum of ocean waves in deep water.

The detailed description of the instrumentation including the buoy and of the observational procedures has been given elsewhere (Mitsuyasu *et al.*, 1973a), and will not be repeated here, though a condensed description of the mathematical procedures for the data analysis is given in this paper.

2. Wave data

Waves were measured by using a cloverleaf buoy. The cloverleaf buoy developed in our laboratory in 1971 is almost the same as that of the National Institute of

Oceanography (Cartwright and Smith, 1964). It can measure the vertical acceleration η_{tt}, slope η_x, η_y, and curvature η_{xx}, η_{yy}, η_{xy} of the wave surface $\eta(t,x,y)$.

From approximately 50 cases, only five typical data sets (identified as Nos. 213, 430, 440, 530 and 550) have been analyzed; each is a continuous record of about 1 h. Fig. 1 shows the locations and dates of the wave observations.

Data sets 213, 530 and 550 correspond to wave data in open seas and data sets 430 and 440, to those for a bay.

Table 1 gives the wind direction θ_w, speed U, and approximate duration t_d, which have been measured from the tending ship near each observation station; H and T are the significant wave height and period, respectively, measured by the cloverleaf buoy.

The wind speeds measured at the observation stations have been determined by taking the mean of the measured wind speeds during the duration. The synoptic charts for the weather situations are shown in the Appendix.

3. Analysis of the wave data

Original wave data recorded on magnetic tapes in analogue form were digitized by using a high-speed A-D converter. The spectral analysis of the data was done on the computer system FACOM 270-20 using a standard program based on fast Fourier transform procedures.

Fundamentals of the mathematical procedure of the data analysis are almost the same as those used by Longuet-Higgins *et al.* (1963) and by Cartwright and Smith (1964).

a. Cross spectral analysis

Cross spectra $C_{lm}(f)-iQ_{lm}(f)$ were computed using the measured six signals from the ocean waves, i.e., the vertical acceleration of wave surface, $\eta_{tt}(=S_1)$, the wave slope, $\eta_x(=S_2)$, $\eta_y(=S_3)$, and the wave curvature $\eta_{xx}(=S_4)$, $\eta_{yy}(=S_5)$, $\eta_{xy}(=S_6)$, as

$$C_{lm}(f)-iQ_{lm}(f)=\int_{-\infty}^{\infty}\overline{S_l(t)S_m(t+\tau)}\exp(i2\pi f\tau)d\tau), \quad l, m=1, 2, \ldots, 6, \quad (1)$$

where

$$\overline{S_l(t)S_m(t+\tau)}=\lim_{T\to\infty}\frac{1}{T}\int_0^T S_l(t)S_m(t+\tau)dt. \quad (2)$$

In the above f is frequency and τ time lag.

For the computation of the cross spectra, the following values apply.

Sampling interval: $\Delta t=0.4$ s
Data points (for one sub-sample): $N=2048$
Sample length (for one sub-sample): $T_N\approx 13.6$ min

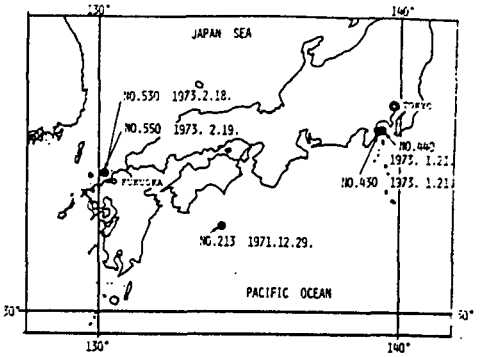

FIG. 1. Locations and dates of the wave observations.

Nyquist frequency: $f=1.25$ Hz
Spectral analysis: FFT method
Elementary frequency bandwidth:
$\Delta f_0=1.22\times10^{-3}$ Hz
Spectral filter (triangular): $\Delta f_c=3.66\times10^{-2}$ Hz
Equivalent degrees of freedom (for one sub-sample):
$\nu=60$

Usually three sub-samples are used for each data set. Therefore, the equivalent degrees of freedom for the measured cross spectra are approximately 180.

b. Computations of the directional spectrum

The directional spectrum $E(f,\theta)$ is conveniently expressed in the form

$$E(f,\theta)=\phi_1(f)G(f,\theta), \quad (3)$$

where $\phi_1(f)$ is the one-dimensional wave spectrum and $G(f,\theta)$ an angular distribution function. The one-dimensional spectrum $\phi_1(f)$ is determined from the acceleration spectrum $C_{11}(f)$, i.e.,

$$\phi_1(f)=(2\pi f)^{-4}C_{11}(f). \quad (4)$$

An angular distribution function $h(f,\theta)$ $[=\pi G(f,\theta)]$ is used tentatively in the present paper.

The coefficients A_n and B_n in the Fourier expansion of $h(f,\theta)$,

$$A_n+iB_n=\frac{1}{\pi}\int_0^{2\pi}h(f,\theta)\exp(in\theta)d\theta, \quad (5)$$

TABLE 1. Wave parameters from the five data sets.

Data set	θ_w	Parameter U (m s^{-1})	t_d (h)	H (m)	T (s)	H/L
213	E-NE	10	26	1.49	6.20	0.025
430	ENE-NE	7	2	0.80	4.45	0.026
440	ENE-NE	7	4	0.74	4.11	0.028
530	NNE	9	4	0.84	4.50	0.027
550	N-NE	10	24	2.34	8.30	0.022

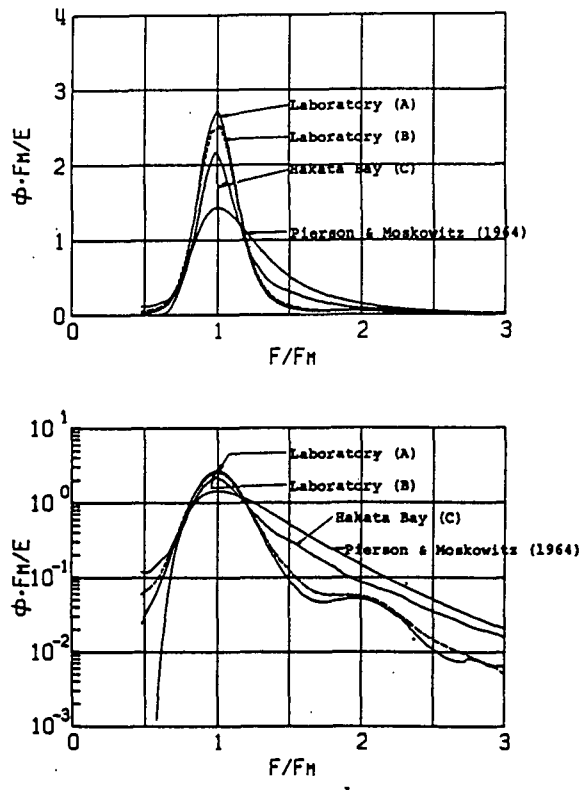

FIG. 2. Similarity of the one-dimensional wave spectrum.

can be determined up to $n=4$, from the measured cross-spectral elements C_{lm} and Q_{lm} where only 17 of the 36 possible cross-spectral elements between the six signals are used. From these Fourier coefficients the angular distribution function $h(f,\theta)$ can be expressed approximately as

$$h_4(f,\theta)=\tfrac{1}{2}+\sum_{n=1}^{4} w_n(A_n\cos n\theta+B_n\sin n\theta), \qquad (6)$$

$$\text{for}\quad \begin{cases} w_1=8/9, & w_2=28/45 \\ w_3=56/165, & w_4=14/99 \end{cases}$$

where the weights w_n are introduced to make $h_4(f,\theta)$ non-negative. The partial Fourier sum with the weights w_n corresponds to the smoothed average of $h(f,\theta)$ by the weighting function $W_4(\theta)$ which is very approximately proportional to $\cos^{16}\theta/2$ and has an rms width $\pm 29°$.[1]

4. Results

a. *One-dimensional spectra of ocean waves*

In a previous study one of the present authors studied the similarity of the one-dimensional spectra of wind-generated waves by using accurately measured wave data for three different groups A, B and C (Mitsuyasu *et al.*, 1973c). The wave data for group A were obtained in a wind-wave facility 1.8 m wide, 3 m deep and 80 m long, with a 20 m closed test section where the height of air gap is 0.65 m. The wave data for group B were obtained in a wave tank 8 m wide, 3 m deep, 80 m long which has a wind blower (outlet mouth: width 4 m ×height 0.4 m) at the middle part of the wave tank. In the latter case, wind waves in the test section were generated by wind which is not restricted by side walls and a ceiling. The wave data of group C were obtained in Hakata Bay, where the water depth is approximately 5 m and the fetch is approximately 5 km to the north.

It was found that wave spectra normalized in the form

$$\frac{\phi_1(f)f_m}{E}=\phi\left(\frac{f}{f_m}\right) \qquad (7)$$

were quite similar and stable within each the groups; here f_m is the spectral peak frequency and E the total energy of the wave spectrum is defined by

$$E=\int_0^\infty \phi_1(f)df=\int_0^\infty\int_0^{2\pi} E(f,\theta)d\theta df. \qquad (8)$$

Moreover, there were no differences in the normalized spectra between groups A and B. However, the normalized spectra of group C were slightly different from those of groups A and B. These results can be clearly seen in Fig. 2 which is reproduced from the previous paper (Mitsuyasu *et al.*, 1973c), and shows the mean form of the normalized spectra of each group together with the normalized spectrum of Pierson and Moskowitz (1964). As can be seen from Fig. 2, the concentration of the normalized spectral energy near the spectral peak is lower in the data of group C than in those of groups A and B. The concentration of the normalized spectral energy of the Pierson-Moskowitz spectrum is much smaller than that of group C. The dimensionless fetch gF/u_*^2 is approximately 10^2–10^3 for the wave data of groups A and B, 10^5–10^6 for those of group C, and approximately 10^7 for the Pierson-Moskowitz spectrum. Therefore, within the range of our previous data, it was concluded that the concentration of the normalized spectral energy of wind waves seems to decrease with increasing dimensionless fetch gF/u_*^2.

In order to check the results of our previous study using the present data of ocean waves under various conditions, all of the measured spectra were normalized in the form of Eq. (7) and compared with the previous results. Some typical examples of the normalized forms of the measured wave spectra are shown in Figs. 3–5. In the upper part of each figure the one-dimensional normalized spectrum is shown on a linear scale and in the lower part of the figure the same spectrum is shown on a semi-logarithmic scale in order to show the details of the measured spectrum at low and high frequencies where the spectral densities are relatively small.

[1] Additional weights w_5–w_8 are necessary in Eq. (6) for the perfect fit to the weighting function of the form $\cos^{16}\theta/2$. However, the error in neglecting these weights is negligible.

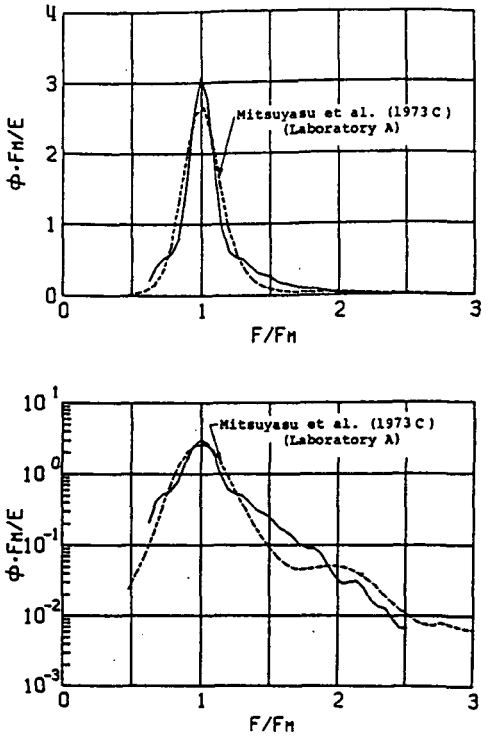

FIG. 3. Normalized form of the one-dimensional wave spectrum: continuous curve, ocean wave data set No. 430/1; dashed curve, laboratory wave data (group A).

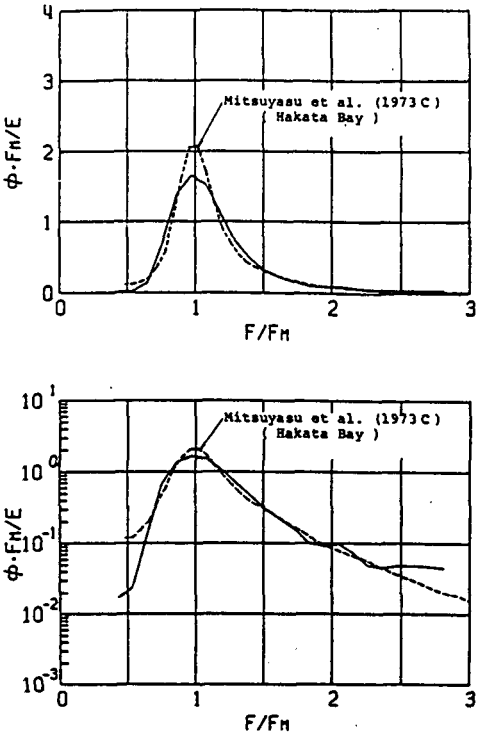

FIG. 4. As in Fig. 3 except for ocean wave data set No. 550/1, and the wave data of Hakata Bay (group C).

The dashed line in each figure shows the spectral form which is selected from the typical spectra shown in Fig. 2 and which has the closest resemblance to each measured spectrum. It can be seen from these figures that the wave spectrum of No. 430/1 is quite similar to the spectrum of laboratory wind waves, the wave spectrum of No. 550/1 is quite similar to the spectrum observed in Hakata Bay, and the wave spectrum of No. 213/1 is quite similar to the Pierson-Moskowitz spectrum. All of the other spectra were scattered between the spectral form for laboratory wind waves and that of Pierson and Moskowitz (1964), though they are not shown in the figures. Furthermore, within the range of our observed spectra, it was shown that the Pierson-Moskowitz spectrum is the spectrum with the smallest energy concentration, in other words, the spectrum with the largest spectral width. Within the range of the present data, however, a definite relation between the normalized spectral form and the dimensionless fetch has not been obtained. Recently, a new spectral form, the JONSWAP spectrum, has been reported (Hasselmann *et al.*, 1973). The JONSWAP spectrum has very high concentration of normalized spectral energy, which is comparable to that for laboratory wind waves. The wave spectrum of No. 430/1 shown in Fig. 3 is very close to the JONSWAP spectrum, though the others shown in Figs. 4 and 5 are different from the JONSWAP spectrum.

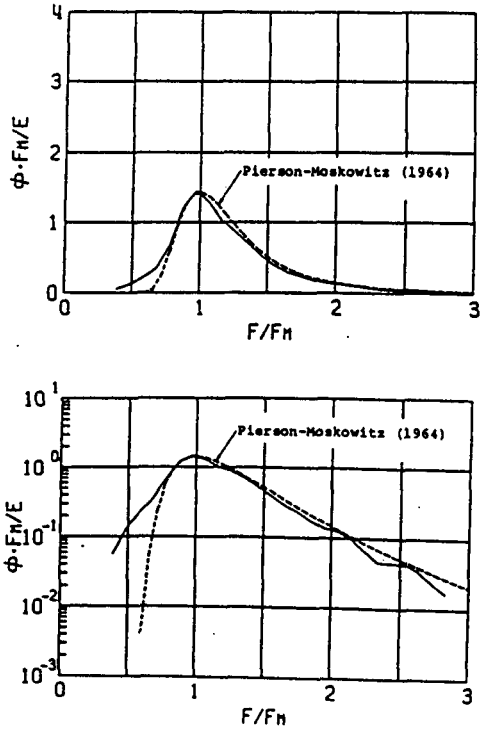

FIG. 5. As in Fig. 3 except for ocean wave data set No. 213/1, and the Pierson-Moskowitz spectrum.

b. The angular distribution function

Fig. 6 shows an example of the measured angular distribution $h_4(f,\theta)$, together with $h_2(f,\theta)$ which is given by

$$h_2(f,\theta)=\tfrac{1}{2}+\sum_{n=1}^{2} w_n'(A_n\cos n\theta+B_n\sin n\theta) \qquad (9)$$

$$\text{for}\quad \begin{cases} w_1'=\tfrac{2}{3}, \\ w_2'=\tfrac{1}{6}. \end{cases}$$

Here, $h_2(f,\theta)$ is an angular distribution which can be determined only from the signals of η_u, η_x and η_y, and corresponds to the data measured by a "pitch-roll buoy." Eq. (9), the partial Fourier sum with weights w_n', corresponds to the smoothed average of $h(f,\theta)$ by the weighting function $W_2(\theta)$ which is proportional to $\cos^4\theta/2$. Since the width of $W_2(\theta)$ is approximately twice as large as that of $W_4(\theta)$, $h_2(f,\theta)$ is smoother than $h_4(f,\theta)$ as shown in Fig. 6. In the figure $h(\theta)$ for each frequency component is shown separately.

It can be seen from Fig. 6 that $h(f,\theta)$ can be well approximated by an unimodal distribution function except for some exceptional cases which are considered to be affected by some errors.

In order to investigate $h(f,\theta)$ more quantitatively, the following function, originally proposed by Longuet-Higgins *et al.* (1963), is fitted to the measured angular distributions

$$h(\theta)=G'(s)\,|\cos\tfrac{1}{2}(\theta-\bar\theta)|^{2s}, \qquad (10)$$

where $G'(s)$ is a normalizing function to make

$$\int_0^{2\pi} h(\theta)d\theta=\pi,$$

i.e.,

$$G'(s)=2^{2s-1}\times\frac{\Gamma^2(s+1)}{\Gamma(2s+1)}. \qquad (11)$$

The parameter s is, in a general case, a function of the wave frequency f, and $\bar\theta$ is the mean direction defined by

$$\bar\theta=\tan^{-1}B_1/A_1\ [=\tan^{-1}Q_{13}/Q_{12}]. \qquad (12)$$

In Eq. (11) Γ is the gamma function.

The form of $h(\theta)$ given by the above equation is shown in Fig. 7 for different values of s. As can be seen, $h(\theta)$ tends to a narrower distribution with an increase of the parameter s. That is, s can be considered as a parameter which controls the concentration of the directional distribution of the wave energy.

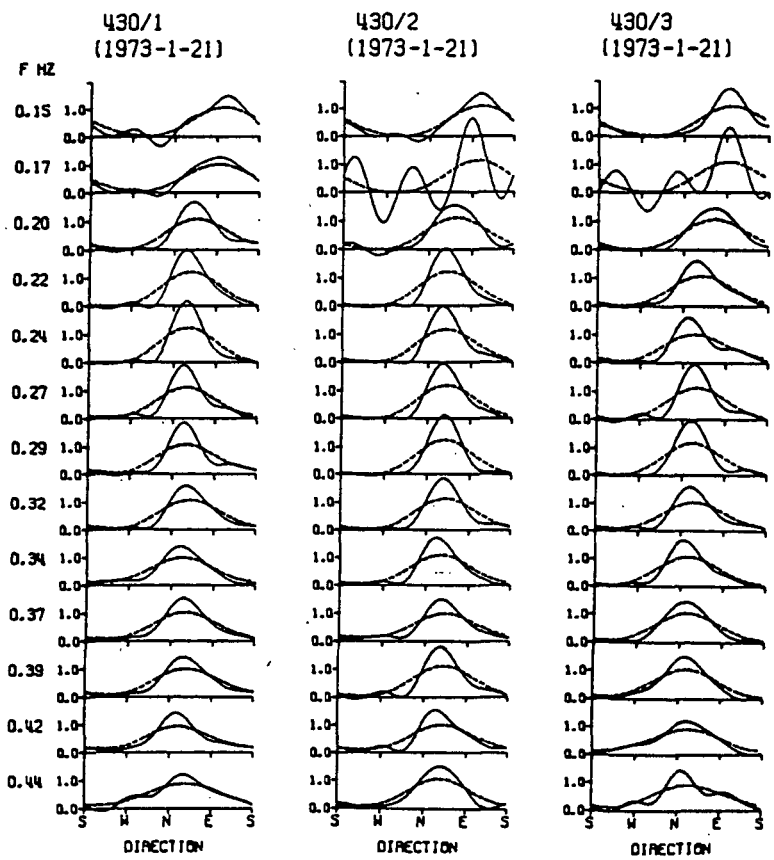

FIG. 6. Angular distribution functions of the directional spectrum (wave data case 430/1,2,3): continuous curve, $h_4(f,\theta)$; dashed curves, $h_2(f,\theta)$.

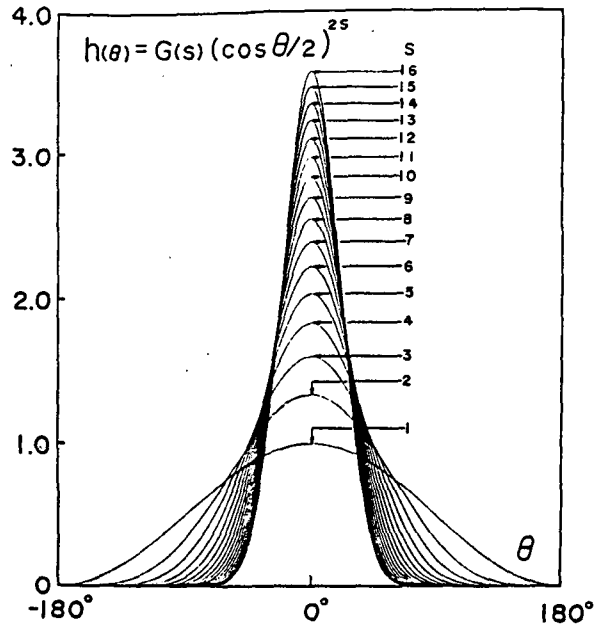

FIG. 7. An idealized angular distribution function.

If Eq. (10) were a perfect fit to the measured angular distribution, the parameter s would have to satisfy all of the expressions

$$C_n=\frac{s(s-1)\cdots(s-n+1)}{(s+1)(s+2)\cdots(s+n)}, \quad n=1, 2, 3, 4, \quad (13)$$

where

$$C_n=(A_n^2+B_n^2)^{\frac{1}{2}}. \quad (14)$$

Eq. (13) implies that definite relations exist among the different C_n by taking s as a parameter. The relations between the measured values of C_1 and C_2 and also C_1 and C_3 are shown in Fig. 8 for the three cases 213/1, 2, 3, together with the relationship implied by Eq. (13). It can be seen that the measured relationship between C_1 and C_2 is very close to the hypothetical curve. However, there is a tendency for C_3 to be relatively too large, although the relation between C_1 and C_3 does not differ appreciably from the hypothetical curve. Similar results have also been obtained for the other data analyzed in this study. Therefore, Eq. (10) can be considered as a fairly good approximation for the measured angular distribution functions.

By using Eqs. (13) and (14) the parameter s_n can be determined from the corresponding Fourier coefficients A_n and B_n, respectively, for $n=1, 2, 3, 4$. Furthermore, if Eq. (10) were a perfect fit to the measured angular distributions, all s_n ($n=1, 2, 3, 4$) should be equal. In fact, s_2 was found to be approximately equal to s_1 as was also to be expected from the results shown in Fig. 8. However, s_3 and s_4 were somewhat different from s_1 and s_2. These might be attributed to the fact that the higher terms of the Fourier coefficients of angular distribution function contain non-negligible errors, due to the poor accuracy in the measurement of wave curvature. Therefore, the parameter s_1 and s_2 will be used for the following discussions.

Figs. 9 and 10 show typical sets of values of $\phi_1(f)$, $\bar{\theta}$, s_1 and s, where s is the mean of the values of s_1 and s_2. The location of the arrow shows the frequency of the maximum spectral density. It can be seen from these figures that the value of s_1 or s is very large near the maximum spectral density frequency. However, it decreases rapidly toward higher and lower frequencies. In other words, the angular distribution is very narrow for the frequency components near the spectral peak frequency, whereas it widens rapidly toward higher and

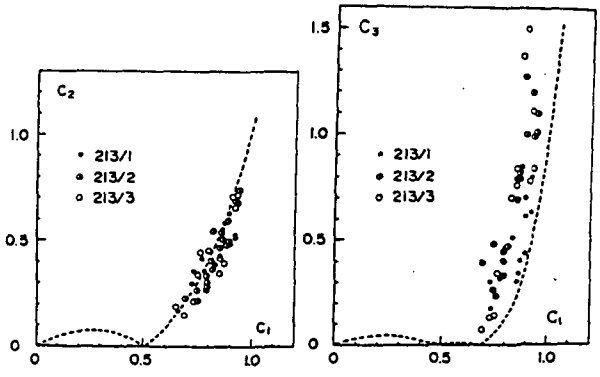

FIG. 8. Relations between measured angular harmonic amplitudes C_1 and C_2 and between C_1 and C_3, and the theoretical relation (dotted lines) according to Eq. (13), for wave cases 213/1,2,3.

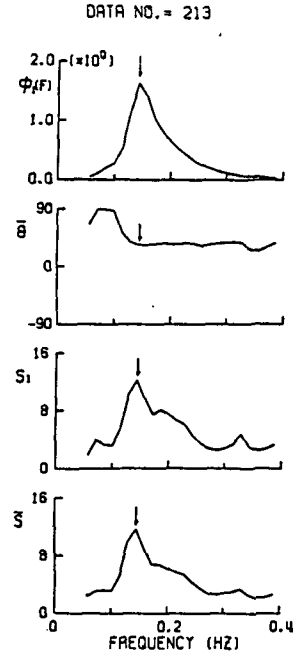

FIG. 9. The one-dimensional wave spectrum $\phi_1(f)$, mean direction $\bar{\theta}$, and the spreading parameters s_1 and s for wave data set 213.

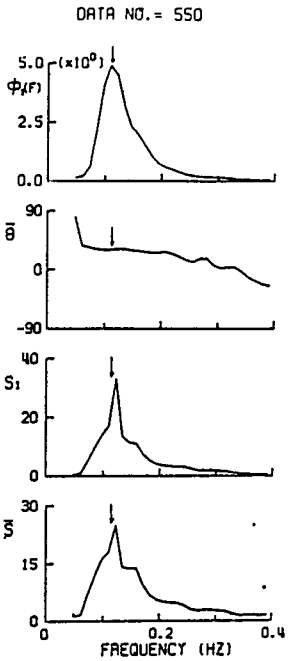

FIG. 10. As in Fig. 9 except for wave data set 550.

lower frequencies. It can also be seen that the mean direction of the dominant spectral component is almost the same as that of the wind (cf. Table 1). Similar results have been obtained from the other sets of data.

Therefore, it can be said that in a generating area, frequency components near the dominant peak of the frequency spectrum, i.e., the most energy-containing frequency components, propagate in almost the same direction as the wind direction and their angular spread is very narrow. However, the angular spreading increases toward higher and lower frequencies as the spectral energy decreases.

Similar properties for the angular spread of the ocean wave spectra can be seen also from the "long-crestedness" parameter

$$\gamma(\tilde{f})=\left(\frac{1-C_2}{1+C_2}\right)^{\frac{1}{4}}, \tag{15}$$

where $\tilde{f}$ is a dimensionless frequency defined as

$$\tilde{f}=2\pi fU/g(=U/C). \tag{16}$$

The long-crestedness parameter $\gamma(\tilde{f})$ is another measure of angular spread of the spectrum introduced by Longuet-Higgins *et al.* (1963). When the spectrum is narrow, $\gamma(\tilde{f})$ is almost equal to the rms angular deviation of energy in the spectrum.

Fig. 11 shows our measured long-crestedness parameter $\gamma(\tilde{f})$ as the function of the dimensionless frequency $\tilde{f}$. The arrow shows the location of the spectral peak frequency of each datum, and the curve inserted in the figure is the theoretical curve

$$\gamma(\tilde{f})=\left[\frac{0.75-0.41Q(\tilde{f})}{1.25+0.41Q(\tilde{f})}\right]^{\frac{1}{4}}, \tag{17}$$

where

$$Q(\tilde{f})=\exp(-\tfrac{1}{2}\tilde{f}^4),$$

which is derived from the SWOP spectrum (Coté *et al.*, 1960). It can be seen from Fig. 11 that the measured values of $\gamma(\tilde{f})$ show a change similar to that of the SWOP curve at the high-frequency part. However, for the low-frequency part the present results are inconsistent with the SWOP curve. That is, there is a minimum value of $\gamma(\tilde{f})$ at some particular frequency which is near the spectral peak frequency of each spectrum; and as $\tilde{f}$ decreases beyond that frequency, $\gamma(\tilde{f})$ increases rapidly again. Therefore, the same conclusion as that obtained with the parameter s can also be obtained from the behavior of $\gamma(\tilde{f})$. That is, the angular spread of the wave spectrum is very narrow near the spectral peak frequency.

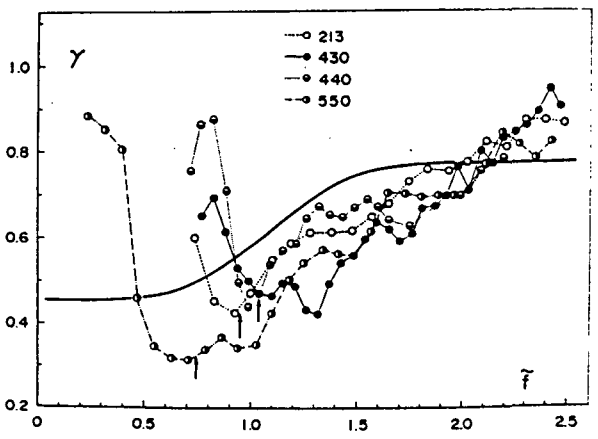

FIG. 11. The long-crestedness parameter $\gamma(\tilde{f})$, compared with the SWOP curve (solid curve).

5. An idealized form of the angular distribution function

In order to find the relation between the parameter s and the dimensionless frequency $\tilde{f}[=2\pi fU/g=U/C]$, $s[=(s_1+s_2)/2]$ and $\tilde{f}$ are plotted in Fig. 12 on a log-log scale. It can be seen that values of the parameter s are almost uniquely determined from the dimensionless frequency $\tilde{f}$ on the high-frequency side of the spectrum, although the data are somewhat scattered due to the insufficient accuracy of the measurements. In Fig. 12 the arrow marks the location of the dimensionless frequency $\tilde{f}_m$ that corresponds to the spectral peak frequency f_m. It can also be seen from Fig. 12 that in each spectrum the parameter s shows its maximum value near $\tilde{f}_m$ as already shown in Figs. 9 and 10, and s decreases rapidly with decreasing $\tilde{f}$ at $\tilde{f}<\tilde{f}_m$. Similar results can also be obtained from the data on s_1.

These facts suggest that for the high-frequency side of the spectrum the parameter s shows an equilibrium

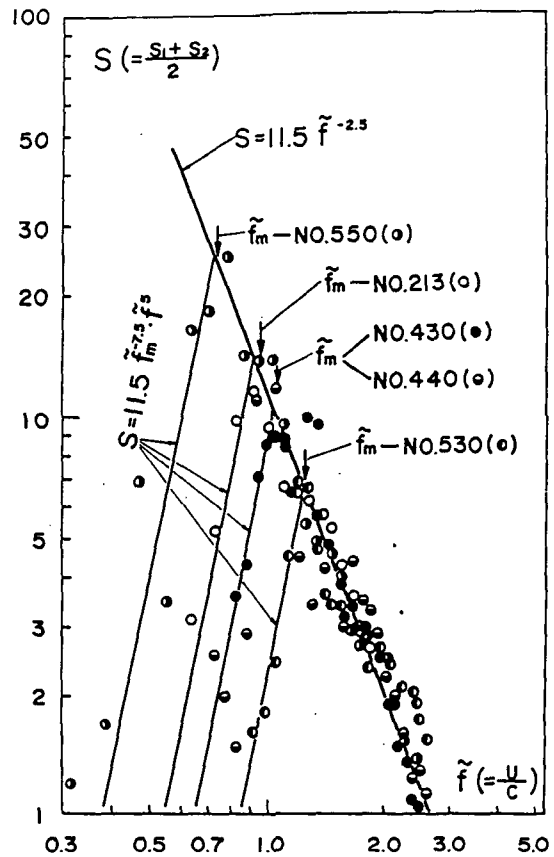

FIG. 12. The parameter s as a function of the dimensionless frequency $\tilde{f}$. $\tilde{f}_m$ is the dimensionless frequency of the maximum density of the one-dimensional wave spectrum.

form which is given approximately by

$$s=11.5\tilde{f}^{-2.5}. \tag{19}$$

In the frequency range below the spectral peak, $f<\tilde{f}_m$, an approximate expression for s can be given by

$$s=k\tilde{f}^m, \tag{20}$$

where k and m are dimensionless constants. The power m in the above expression seems to depend somewhat on $\tilde{f}_m$. That is, as shown in Fig. 12, m is slightly larger in the cases of smaller $\tilde{f}_m$ than in those of larger $\tilde{f}_m$. At this time, however, these differences in m are neglected and m is assumed to be

$$m=5.$$

The constant k can be determined from the condition that s has its maximum value s_m at $\tilde{f}_m$ where Eq. (20) coincides with Eq. (19).

Approximate expressions for s for $\tilde{f}\lesssim\tilde{f}_m$ and for s_m are

$$s=11.5\,\tilde{f}_m^{-7.5}\tilde{f}^5, \tag{21}$$

$$s_m=11.5\,\tilde{f}_m^{-2.5}. \tag{22}$$

On the other hand, the dimensionless frequency $\tilde{f}_m$ of the spectral peak can be determined from the dimensionless fetch $\tilde{F}[=gF/U^2]$ by using the so-called fetch relation. For example, the fetch relation (Mitsuyasu 1968)

$$\hat{f}_m=1.00\,\hat{F}^{-0.330}, \tag{23}$$

where

$$\hat{f}_m=u_*f_m/g, \quad \hat{F}=gF/u_*^2, \tag{24}$$

where u_* is the friction velocity of the wind, can be transformed into

$$\tilde{f}_m=18.8\,\tilde{F}^{-0.330} \tag{25}$$

by using the approximate relation

$$25\,u_*=U_{10}=U. \tag{26}$$

From Eqs. (10), (19), (21) and (25) we can derive an idealized form of the angular distribution function that can be used for practical purposes. That is, the angular distribution is given by

$$G_1(\tilde{f},\theta)=G_1'(s)\,|\cos\theta/2|^{2s}, \tag{27}$$

where

$$G_1'(s)=\frac{1}{\pi}2^{2s-1}\frac{\Gamma^2(s+1)}{\Gamma(2s+1)}. \tag{28}$$

The parameter s is given by Eq. (19) for $\tilde{f}\gtrsim\tilde{f}_m$ and by Eq. (21) for $\tilde{f}\lesssim\tilde{f}_m$, and $\tilde{f}_m$ can be determined from Eq. (25).

From Eqs. (19), (21) and (22) the other expressions for s are as follows:

$$s/s_m=(\tilde{f}/\tilde{f}_m)^{-2.5}, \quad \text{for } \tilde{f}\gtrsim\tilde{f}_m, \tag{29}$$

$$s/s_m=(\tilde{f}/\tilde{f}_m)^{5}, \quad \text{for } \tilde{f}\lesssim\tilde{f}_m. \tag{30}$$

It should be mentioned here that the parameter s at the spectral peak frequency $\tilde{f}_m$ increases with an increase in the dimensionless fetch $\tilde{F}$. In other words, the angular distribution becomes narrower as the dimensionless fetch increases. This is a rather unexpected result, because it would appear that the angular distribution should broaden with increasing fetch due to the fluctuation of the wind direction in a generating area. The result may be due to the properties of the wave motion itself, because the wind action may not be as effective for fully developed waves ($\tilde{f}_m=U/C_m\lesssim1$) in a large fetch, where C_m is the velocity of the dominant wave.

6. Comparison of various angular distribution functions

Finally, the proposed form of the angular distribution function, $G_1(\tilde{f},\theta)$, is compared with the other forms which have been used frequently for practical purposes. Typical forms of the angular distribution are

1. PNJ type (Pierson *et al.*, 1955)

$$G_0(\theta)=\frac{2}{\pi}\cos^2\theta \tag{31}$$

2. SWOP spectrum (Coté *et al.*, 1960)

$$G_3(\tilde{f},\theta)=\begin{cases}\dfrac{1}{\pi}(1+a\cos 2\theta+b\cos 4\theta), & \text{for } |\theta|\leqslant\pi/2\\ 0, & \text{for } |\theta|>\pi/2\end{cases} \tag{32}$$

where

$$a=0.50+0.82\exp(-\tfrac{1}{2}\tilde{f}^4), \tag{33}$$

$$b=0.32\exp(-\tfrac{1}{2}\tilde{f}^4). \tag{34}$$

Figs. 13 and 14 show the comparisons of the various forms for the angular distribution functions, $G_0(\theta)$, $G_1(\tilde{f},\theta)$ and $G_3(\tilde{f},\theta)$, by taking $\tilde{f}[=U/C]$ as a parameter. Here, $G_1(\tilde{f},\theta)$ shown in the figures corresponds to angular distributions of the spectral components in a frequency range $\tilde{f}\gtrsim\tilde{f}_m$. It can be seen from Figs. 13 and 14 that $G_0(\theta)$ is an appropriate form for the spectral components near the frequency $\tilde{f}[=U/C]\approx 1.5$, but it has a wider angular distribution for the frequency components $\tilde{f}<1.5$ and narrower angular distribution for the frequency components $\tilde{f}>1.5$, as compared $G_1(\tilde{f},\theta)$; $G_3(\tilde{f},\theta)$ is very close to $G_1(\tilde{f},\theta)$ for the frequency components $\tilde{f}\approx 1.8$–2.0, although there exist some discontinuities of the distributions at $|\theta|=\pi/2$. Furthermore, $G_3(\tilde{f},\theta)$ shows a wider angular distribution for the frequency components $\tilde{f}<1.8$ and a narrower angular distribution for $\tilde{f}>2.0$.

In some cases the following form of the angular distribution function has been used for practical purposes:

$$G_2(\tilde{f},\theta)=G_2'(n)\cos^n\theta, \tag{35}$$

where

$$G_2'(n)=\frac{1}{\pi^{\frac{1}{2}}}\frac{\Gamma\left(1+\frac{n}{2}\right)}{\Gamma\left(\frac{1}{2}+\frac{n}{2}\right)}. \tag{36}$$

It can be shown by comparing $G_2(\tilde{f},\theta)$ with $G_1(\tilde{f},\theta)$ that

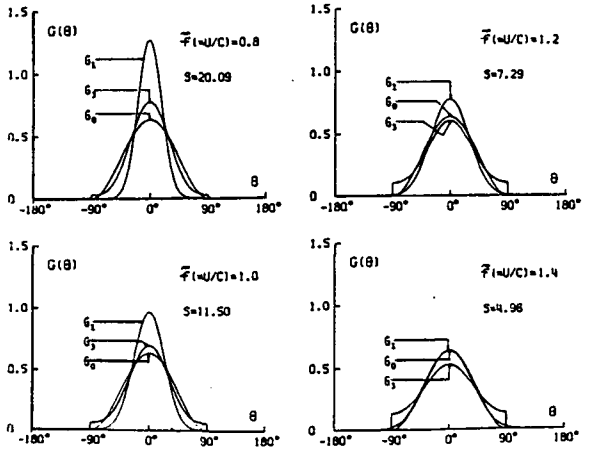

FIG. 13. The angular distribution functions $G_0=(2/\pi)\cos^2\theta$, G_1 (proposed spectrum) and G_3 (SWOP spectrum), as a function of the dimensionless frequency $\tilde{f}$.

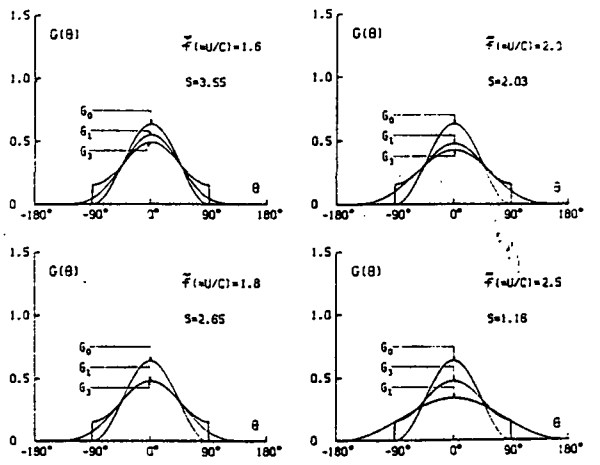

FIG. 14. As in Fig. 13 for other values of $\tilde{f}$.

$G_2(\tilde{f},\theta)$ becomes very close to $G_1(\tilde{f},\theta)$ if we assume

$$n=0.46s, \tag{37}$$

and use Eqs. (19) and (21) for the values of s. The relation (37) is only an approximate relation which gives consistent results for the frequency components $\tilde{f}\lesssim 1.6$ or $s\gtrsim 4$.

7. Conclusions

Using typical wave data measured by the cloverleaf buoy we have determined the directional spectrum of ocean waves, in particular, the form of the one-dimensional frequency spectrum and that of the angular distribution function. While final conclusions have not been obtained for the frequency spectrum, an idealized form of the angular distribution function has been determined, which can be used for practical purposes.

The most important findings of the present study are the following properties of the angular distribution of wave energy. The angular distribution is very narrow for the frequency components near the spectral peak, whereas it widens toward high and low frequencies. Furthermore, the angular distributions of the frequency components near the spectral peak become narrower with increasing dimensionless fetch and, thus, with the growth of the wind waves. These properties are included in the proposed form of the idealized angular distribution function.

Acknowledgments. We would like to acknowledge our debt to Mitsui Ocean Development Company, Ocean Research Institute of Tokyo University, and Navigation Training Establishment of Ministry of Transportation, for allowing us the generous use of their ships, *Aotaka*, *Tansei Maru* and *Shintoku Maru*, respectively. We are also indebted to the captains and crews of these ships for expert handling of both the ships and the buoy in rough seas. We also wish to acknowledge the many engineers in the Research Institute for Applied Mechanics, especially Mr. K. Eto and Mr. T. Kita, for their constant support in the wave observations, Mr.

M. Tanaka for the processing of a great amount of buoy records, Mr. M. Takagi and Mr. H. Hiyama for their assistance in the design and test of the buoy, and Miss N. Uraguchi for typing the manuscript. Finally we are grateful to Dr. W. J. Pierson, Prof. R. O. Reid and Dr. J. A. Ewing for helpful comments on a first draft of this paper. The work described in this paper is part of a special project supported by the Ministry of Education, Japan.

APPENDIX

Synoptic Charts of the Weather Situations

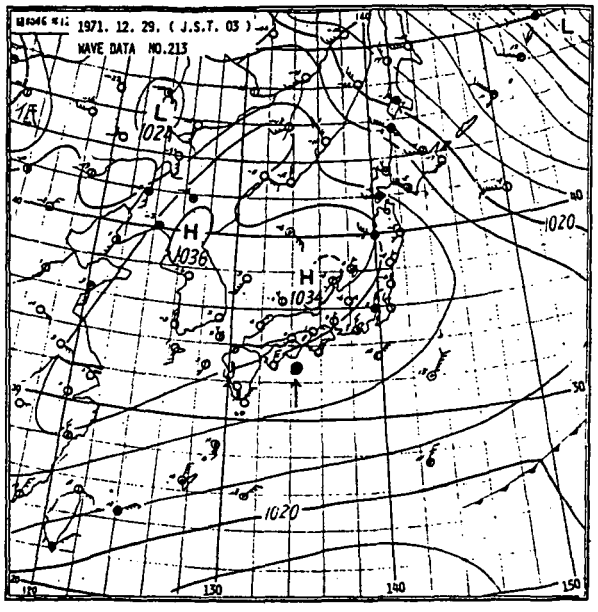

FIG. A1. Surface synoptic map for 0300 JST 29 December 1971 (wave data set No. 213).

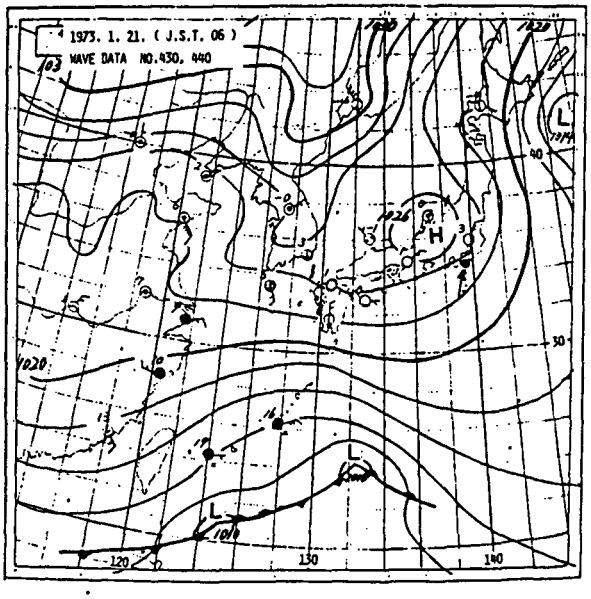

FIG. A2. Surface synoptic map for 0600 JST 21 January 1973 (wave data sets No. 430 and No. 440).

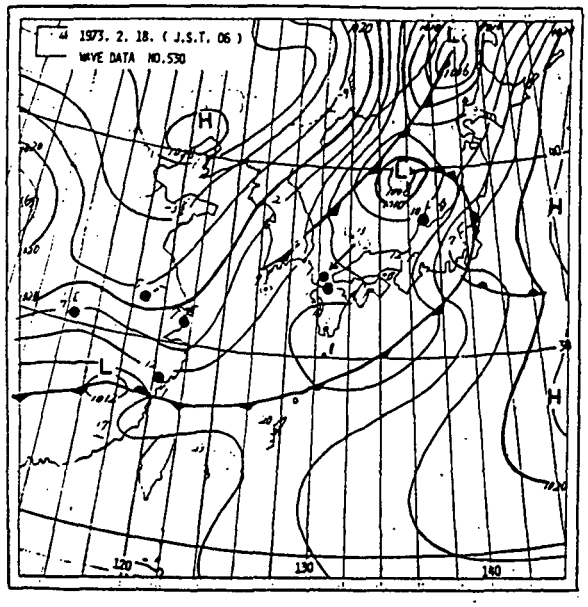

FIG. A3. Surface synoptic map for 0600 JST 18 February 1973 (wave data set No. 530).

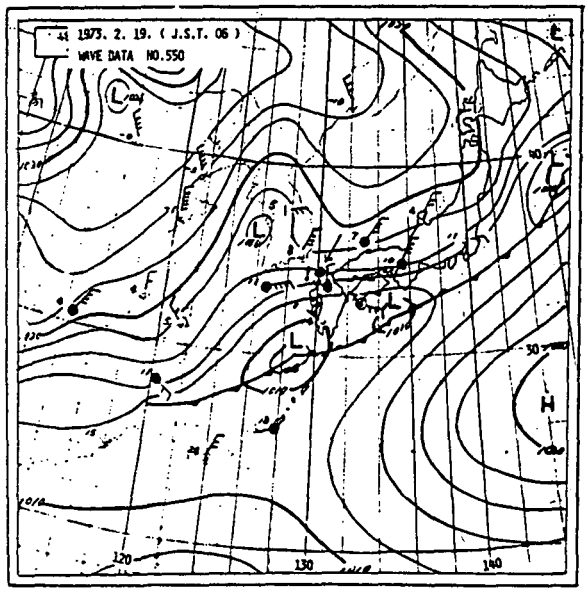

FIG. A4. Surface synoptic map for 0600 JST 19 February 1973 (wave data set No. 550).

REFERENCES

Cartwright, D. E. and N. D. Smith, 1964: Buoy techniques for obtaining directional wave spectra. *Buoy Technology*, Washington, D.C., Marine Tech. Soc., 112–121.

Coté, L. J., J. O. Davis, W. Marks, R. J. McGough, E. Mehr, W. J. Pierson, Jr., J. F. Ropek, G. Stephenson and R. C. Vetter, 1960: The directional spectrum of a wind-generated sea as determined from data obtained by the Stereo Wave Observation Project. *Meteor. Papers*, 2, No. 6, New York University, 88 pp.

Ewing, J. A., 1969: Some measurements of the directional wave spectrum. *J. Marine Res.*, 27, 163–171.

Hasselmann, K. *et al.*, 1973: Measurements of wind-wave growth and swell decay during the Joint North Sea Wave Project (JONSWAP). *Deut. Hydrogr. Z*, 12, 1–95.

Longuet-Higgins, M. S., D. E. Cartwright and N. D. Smith, 1963: Observations of the directional spectrum of sea waves using the motions of a floating buoy. *Proc. Conf. Ocean Wave Spectra*, Prentice-Hall, 111–132.

Mitsuyasu, H., 1968: On the growth of the spectrum of wind-generated waves (1). *Rep. Res. Inst. Appl. Mech. Kyushu Univ.*, 16, No. 55, 459–482.

——, F. Tasai, T. Suhara, S. Mizuno, M. Ohkusu, T. Honda, K. Rikiishi, M. Takagi and H. Hiyama, 1973a: Studies on techniques for ocean wave measurements (1). *Bull. Res. Inst. Appl. Mech., Kyushu Univ.*, No. 39, 105–181.

——, ——, ——, ——, ——, —— and ——, 1973b: Studies on techniques for ocean wave measurements (2). *Bull. Res. Inst. Appl. Mech., Kyushu Univ.*, No. 40, 295–329.

——, ——, J. Okabe, T. Suhara, S. Taneda and T. Honda, 1973c: Laboratory simulation of ocean waves. *Bull. Res. Inst. Appl. Mech., Kyushu Univ.*, No. 39, 183–210.

Pierson, W. J. and L. Moskowitz, 1964: A proposed spectral form for fully developed wind seas based on the similarity theory of S. A. Kitaigorodskii. *J. Geophys. Res.*, 69, 5191–5203.

——, G. Neumann and R. W. James, 1955: Practical methods for observing and forcasting ocean waves by means of wave spectra and statistics. H. O. Publ. 603, U. S. Navy Hydrographic Office.

Tyler, G. L. *et al.*, 1974: Wave directional spectra from synthetic aperture observations of radio scatter. *Deep-Sea Res.*, 22, 987–1016.